ACS central science

Research Article

http://pubs.acs.org/journal/acscii

1,6-Cyclophellitol Cyclosulfates: A New Class of Irreversible Glycosidase Inhibitor

Marta Artola,[†] Liang Wu,[‡] Maria J. Ferraz,[§] Chi-Lin Kuo,[§] Lluís Raich,[∥] Imogen Z. Breen,[‡] Wendy A. Offen,[‡] Jeroen D. C. Codée,[†] Gijsbert A. van der Marel,[†] Carme Rovira,[∥,⊥] Johannes M. F. G. Aerts,[§] Gideon J. Davies,*[,‡] and Herman S. Overkleeft*[,†]

[†]Department of Bio-organic Synthesis and [§]Department of Medical Biochemistry, Leiden Institute of Chemistry, Leiden University, P.O. Box 9502, 2300 RA Leiden, The Netherlands

[‡]Department of Chemistry, University of York, Heslington, York, YO10 5DD, U.K.

[∥]Departament de Química Inorgànica i Orgànica (Secció de Química Orgànica) and Institut de Química Teòrica i Computacional (IQTCUB), Universitat de Barcelona, Martí i Franquès 1, 08028 Barcelona, Spain

[⊥]Fundació Catalana de Recerca i Estudis Avançats (ICREA), Passeig Lluís Companys 23, 08010 Barcelona, Spain

Supporting Information

ABSTRACT: The essential biological roles played by glycosidases, coupled to the diverse therapeutic benefits of pharmacologically targeting these enzymes, provide considerable motivation for the development of new inhibitor classes. Cyclophellitol epoxides and aziridines are recently established covalent glycosidase inactivators. Inspired by the application of cyclic sulfates as electrophilic equivalents of epoxides in organic synthesis, we sought to test whether cyclophellitol cyclosulfates would similarly act as irreversible glycosidase inhibitors. Here we present the synthesis, conformational analysis, and application of novel 1,6-cyclophellitol cyclosulfates. We show that 1,6-*epi*-cyclophellitol cyclosulfate (α-cyclosulfate) is a rapidly reacting α-glucosidase inhibitor whose $^4C_1$ chair conformation matches that adopted by α-glucosidase Michaelis complexes. The 1,6-cyclophellitol cyclosulfate (β-cyclosulfate) reacts more slowly, likely reflecting its conformational restrictions. Selective glycosidase inhibitors are invaluable as mechanistic probes and therapeutic agents, and we propose cyclophellitol cyclosulfates as a valuable new class of carbohydrate mimetics for application in these directions.

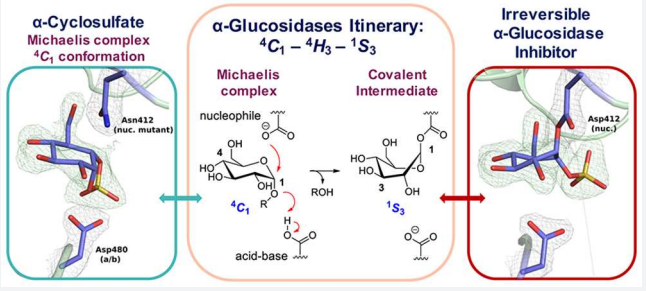

INTRODUCTION

The huge diversity of oligosaccharide, polysaccharide, and glycoconjugate structures found in nature reflect their many roles in biological processes. Such diversity is mirrored in the numerous enzymes that have evolved to degrade these biopolymers. Hydrolytic carbohydrate degrading enzymes, glycoside hydrolases or glycosidases, are classified into over 140 distinct sequence (and hence structural) families in the CAZy database.[1] This classification provides a powerful framework upon which aspects of conformational analysis and enzyme inhibition can be constructed.

Most retaining glycosidases employ a conserved mechanism, in which the acetals (occasionally ketals) that make up interglycosidic linkages are hydrolyzed using two key carboxylic acid residues (Asp or Glu), which function as catalytic nucleophile and catalytic acid/base.[2] Central to glycosidase activity are the considerable conformational distortions undergone by the sugar substrate throughout the catalytic cycle, which are necessary to satisfy the stereoelectronic and orbital overlap requirements for glycoside hydrolysis.[3]

Upon binding to the enzyme, a retaining glycosidase substrate in the Michaelis complex initially adopts a conformation in which the leaving group is axially or pseudoaxially positioned, allowing for favorable in-line attack by the catalytic nucleophile. Nucleophilic attack, with concurrent protonation of the glycosidic oxygen by the catalytic acid/base, leads to a high-energy state (the transition state, TS) with considerable oxocarbenium ion character. This transition state must necessarily adopt a conformation in which C5−O5−C1−C2 are coplanar, to allow for partial oxocarbenium double bond development between O5 and C1. Following this transition state, the substrate forms a covalent intermediate with the glycosidase nucleophile, which is intercepted by water (following the reverse conformational itinerary) to liberate free sugar and enzyme. For retaining α- and β-glucosidases, the typical conformational itineraries for the Michaelis complex → TS → intermediate enzymatic half reactions are $^4C_1 \rightarrow {}^4H_3^{\ddagger} \rightarrow {}^1S_3$ and $^1S_3 \rightarrow {}^4H_3^{\ddagger} \rightarrow {}^4C_1$ respectively (Figure 1a), with the

Received: May 19, 2017
Published: July 13, 2017

DOI: 10.1021/acscentsci.7b00214
ACS Cent. Sci. 2017, 3, 784−793

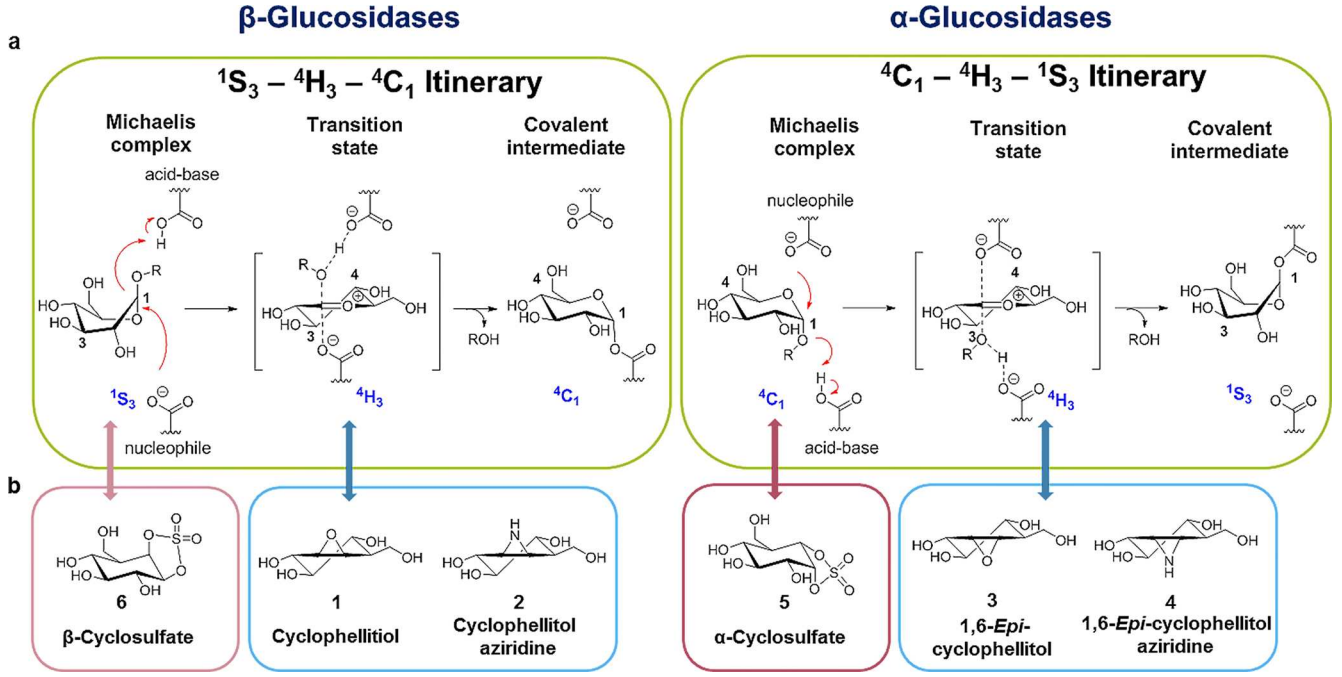

Figure 1. Conformational itinerary of retaining glucosidase reaction pathways and conformation of covalent inhibitors. (a) Reaction itineraries of retaining β-glucosidases and retaining α-glucosidases, showing conformations of the Michaelis complex, transition state, and covalent intermediates. (b) Structures of cyclophellitol (**1**), cyclophellitol aziridine (**2**), 1,6-*epi*-cyclophellitol (**3**), 1,6-*epi*-cyclophellitol aziridine (**4**), α-cyclosulfate (**5**), and β-cyclosulfate (**6**).

$^4H_3$ TS conformation common to both α- and β-glucosidases.[4−7]

Mimicry of transition state features is a powerful strategy for the design of enzyme inhibitors, and thus the majority of competitive glycosidase inhibitors bind by virtue of mimicking either the positive charge or the conformational shape of the transition state.[3,8,9] Conformational mimicry can also aid the reaction of irreversible covalent glycosidase inhibitors,[10] such as cyclitol epoxides and aziridines.[10−12] The natural product, cyclophellitol (**1**), and its synthetic analogue, cyclophellitol aziridine (**2**), are glucose configured inhibitors, which mimic the $^4H_3$ conformation adopted by retaining β-glucosidase substrates in their transition state.[3,13,14] Upon binding to the enzyme active site, nucleophilic attack by the catalytic nucleophile residue opens the epoxide or aziridine ring, irreversibly inhibiting the enzyme via formation of a covalent enzyme−cyclophellitol (aziridine) adduct.

In general, reactive cyclophellitol analogues, locked into TS-like conformations, are rapid irreversible inactivators of retaining glycosidases.[12,15,16] We recently demonstrated that replacement of the cyclophellitol epoxide or aziridine ring by a nonhydrolyzable cyclopropane also yields reversible glycosidase inhibitors with micromolar to nanomolar affinity.[9] Thus, conformation, rather than just electrophilic reactivity, may make a substantial contribution to the inhibitory potency of cyclophellitol analogues.

Given the success of reactive sugar epoxides and aziridines as conformationally enhanced retaining glycosidase inactivators,[10,12,17] we sought to expand the concept to other electrophilic species. Cyclic sulfate electrophiles are often used in synthetic organic chemistry as equivalents of epoxides in nucleophilic additions, sometimes showing superior reactivity and regioselectivity.[18] We therefore sought to test if cyclophellitol configured cyclosulfates could act as a new class of covalent glycosidase inhibitors. Specificity for "α" and "β" enzymes can be conferred simply through choice of the appropriately configured cyclosulfate. We additionally reasoned that substitution of the epoxide in **1** and **3** by a 1,2-*cis*-cyclic sulfate should yield compounds favoring a $^4C_1$ conformation. "α-Configured" 1,6-*epi*-cyclophellitol cyclosulfate **5** (hereafter referred to as α-cyclosulfate) should match, conformationally, the $^4C_1$ Michaelis complex conformation of substrates for α-glucosidases and thus be readily poised for in-line nucleophilic attack by the enzyme, yielding a rapid and potent irreversible inhibitor. In contrast, a "β-configured" 1,6-cyclophellitol cyclosulfate **6** (β-cyclosulfate) locked into a $^4C_1$ conformation would likely disfavor reactivity on retaining β-glucosidases, whose Michaelis complex is $^1S_3$.

Here, we present the synthesis of a panel of 1,6-cyclophellitol cyclosulfates which favor $^4C_1$ chair conformations. α-Cyclosulfate **5** irreversibly inhibits retaining α-glucosidases with affinity on a par with 1,6-*epi*-Cyclophellitol aziridine **4**, whereas β-cyclosulfate **6** is a substantially weaker β-glucosidase inhibitor compared to its cognate aziridine **2**. 3-D structures of covalent adducts from both "α" and "β" cyclosulfates, bound to representative α- and β-glucosidases, combined with inhibitory kinetic studies and competitive activity based protein profiling (ABPP), demonstrate the high specificity and active center−nucleophile reactivity of these molecules.

The development of selective inhibitors of carbohydrate processing enzymes is of major interest both for the understanding of biological processes involved in glycan processing and in the discovery of new therapeutics.[19] Only minor advances have been observed regarding the development of new irreversible glycosidase inhibitors since the discovery of cyclophellitol[20] (aziridines)[21] or 5-fluoro-[22] and 2-deoxy-2-fluoro-[23] glycosides, the latter some 30 years ago.[24] Cyclophellitol cyclosulfates thus provide a conceptually novel and

DOI: 10.1021/acscentsci.7b00214
ACS Cent. Sci. 2017, 3, 784−793

powerful tool for further study of glycosidases in health and disease.

RESULTS AND DISCUSSION

Conformational Free Energy Landscapes of Cyclophellitol Cyclosulfates. Cyclophellitol cyclosulfates **5** and **6** were conceived as putative inhibitors of retaining glucosidases. To determine the likely conformations of these molecules, we first calculated their conformational free energy landscapes (FELs) using *ab initio* metadynamics (Supporting Information).[25] For both **5** and **6**, the calculated ground state conformation was centered at $^4C_1$, with a wide energy minimum expanding toward the $^2H_3$–E_3–$^4H_3$ region (Figure 2a).

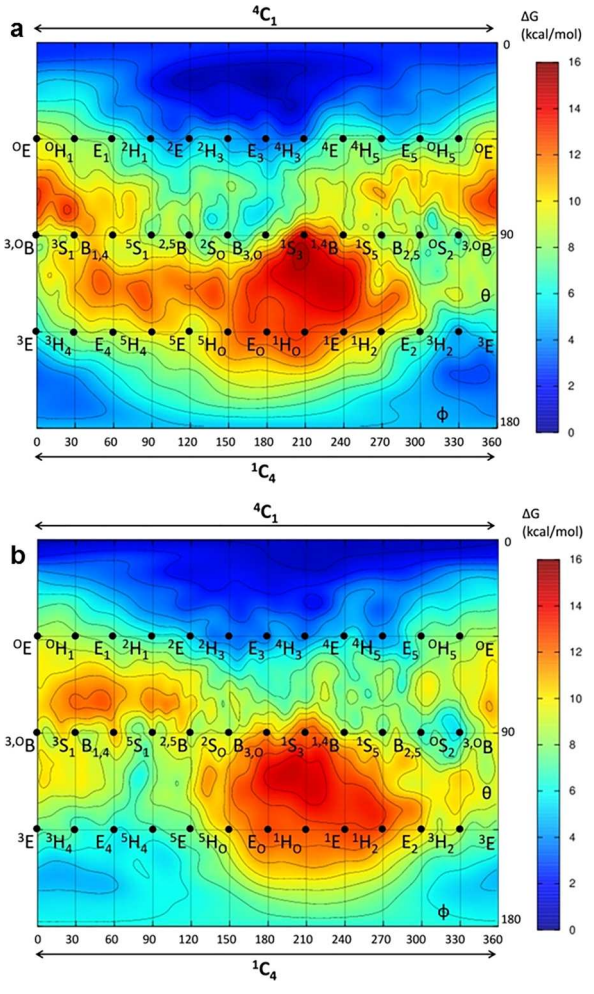

Figure 2. Conformational free energy landscapes of cyclosulfates **5** and **6**. Cyclosulfates **5** (a) and **6** (b) adopt $^4C_1$ ground state conformations, with a broad energy minimum extending toward $^4H_3$. The *x* and *y* axes of each graph correspond to the φ and θ Cremer–Pople puckering coordinates (in degrees), respectively. Isolines are 1 kcal/mol.

We reasoned that the conformational preference of **5** should render it a potent inactivator of α-glucosidases, as its $^4C_1$ conformation matches that of a typical α-glucosidase Michaelis complex, with the $^4H_3$ TS conformation also energetically accessible. In contrast, **6** should not be able to access the $^1S_3$ β-glucosidase Michaelis complex conformation, although the $^4H_3$ TS conformation could still be accessible. Thus, while **6** may still inhibit β-glucosidases, it should do so with less potency compared to **5** vs α-glucosidases.

Synthesis of Cyclic Sulfates 5 and 6. Key intermediate **7** was synthesized from D-xylose in nine steps as optimized in our group based on the total synthesis of cyclophellitol **1** by Madsen and co-workers (Figure 3a).[26,27] Benzylation of the free alcohols in **7** yielded alkene **8**, which was oxidized (ruthenium trichloride/sodium periodate) to afford a mixture of *cis* diols **9** and **10**. Compound **10**, emulating α-glucopyranosides in configuration, was obtained pure after silica gel column chromatography, whereas β-analogue **9** necessitated recrystallization from methanol and diethyl ether in order to obtain homogeneous material. Generation of the cyclic sulfites by treatment of thionyl chloride and subsequent oxidation gave perbenzylated cyclic sulfates **11** and **12**, the benzyl ethers of which were removed by hydrogenolysis using catalytic palladium on carbon to afford compounds **5** and **6**. In line with FEL calculations, analysis of experimental *J*-coupling values for compounds **5** and **6** showed that these analogues indeed adopt a $^4C_1$ conformation in solution (Table S1).

***In Vitro* Inhibition of α- and β-Glucosidases and Kinetic Studies.** To establish the activity of cyclosulfates **5** and **6** in relation to their calculated conformations, we assessed their ability to inhibit representative α- and β-glucosidases compared to cyclophellitol epoxides and aziridines **1**–**4**, utilizing both purified glycosidases and human cell/tissue lysates.

We first tested inhibition against human β-glucosidases GBA1 (recombinant Cerezyme protein from Genzyme, classified into the CAZy glycoside hydrolase family GH30) and GBA2 (GBA2 overexpressing HEK293T lysate, family GH116), and α-glucosidases GAA (recombinant Myozyme from Genzyme, family GH31) and GANAB (Pompe disease fibroblast lysates, family GH31; Table 1). Consistent with our previous findings, cyclophellitol **1** and cyclophellitol aziridine **2** were potent inhibitors of GBA1 and GBA2, and 1,6-*epi*-cyclophellitol **3** and 1,6-*epi*-cyclophellitol aziridine **4** inhibited GAA and GANAB.[10,17,28] In line with our predictions regarding Michaelis complex mimics as strong retaining glycosidase inhibitors, α-cyclosulfate **5** proved to be a potent nanomolar α-glucosidase inhibitor (IC_{50} 82 nM vs GAA; 29 nM vs GANAB) with no reactivity toward β-glucosidases. In contrast, β-cyclosulfate **6** was only a modest inhibitor of β-glucosidases (IC_{50} 119 μM for GBA1 and 58 μM for GBA2). IC_{50}s determined against representative recombinant bacterial glucosidases (β-glucosidases from *Thermotoga maritima*, *Tm*GH1,[3,29] and *Thermoanaerobacterium xylanolyticum*, *Tx*GH116;[30] α-glucosidase from *Cellvibrio japonicus*, *Cj*Agd31B[10,31]) showed the same trend as for the human enzymes: strong inhibition by **5**, and poor inhibition by **6** (Table S2). To confirm that **5** and **6** were stable under the acidic conditions utilized for these enzymatic assays, the solvolytic stability of these compounds in McIlvaine buffer pH 4.0 was assessed by NMR. We observed no spontaneous hydrolysis after 24 h for either **5** or **6** (Figure S2).

We next determined kinetic parameters of inhibition by **1**–**6** against recombinant human GBA1 and GAA, as well as bacterial β-glucosidase *Tm*GH1 (Table 2, Figure S3).[32] Epoxides **1** and **3** irreversibly inhibited GBA and GAA, with initial binding constants (K_I) of 9.2 μM and 1.4 mM, and inactivation rate constants (k_{inact}) of 0.7 and 0.5 min^{-1} respectively. Consistent with their greater reactivity, aziridines **2** and **4** inhibited GBA and GAA considerably faster than epoxides (full inhibition typically within 30 s at higher

DOI: 10.1021/acscentsci.7b00214
ACS Cent. Sci. 2017, 3, 784–793

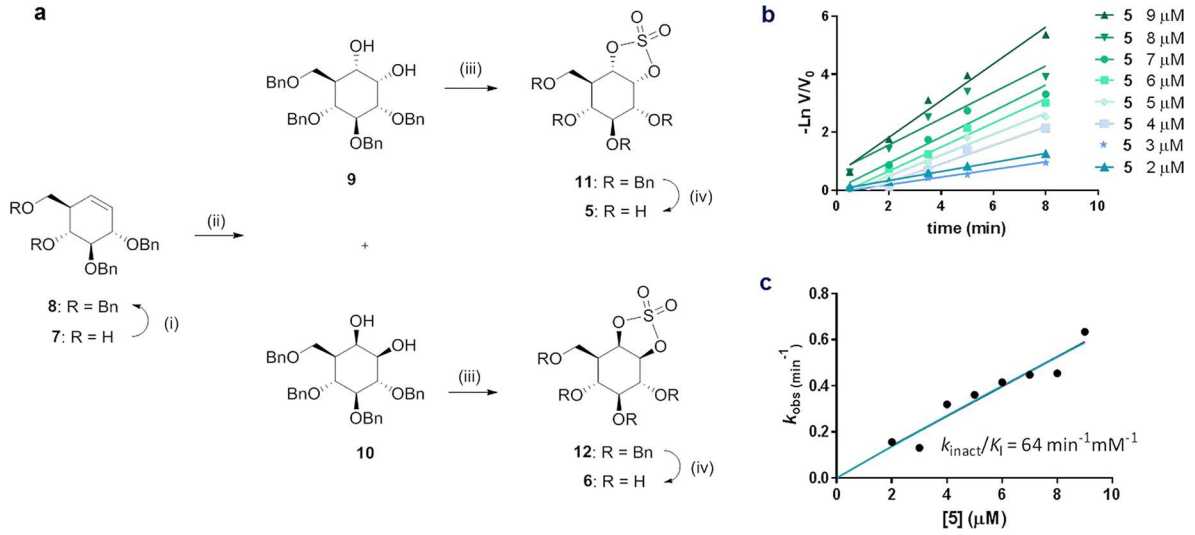

Figure 3. Synthesis of cyclophellitol cyclosulfates **5** and **6**, and inactivation of GAA by compound **5**. (a) Compounds **5** and **6** were prepared from cyclohexene **11**. Reagents and conditions: (i) BnBr, TBAI, NaH, DMF, rt, 18 h, 70%; (ii) $RuCl_3$, $NaIO_4$, EtOAc, ACN, 0 °C, 2 h (**13**, 39%; **14**, 26%); (iii) (a) $SOCl_2$, Et_3N, DCM, 0 °C, (b) $RuCl_3$, $NaIO_4$, CCl_4, ACN, 0 °C, 3 h (**15**, 59%; **16**, 62%); (iv) H_2, Pd/C, MeOH, rt, 18 h (**5**, 71%; **6**, 72%). (b) Semilogarithmic plots of residual activity of GAA versus time at 9, 8, 7, 6, 5, 4, 3, and 2 μM α-cyclosulfate **5**. (c) Plot of pseudo first order rate constants from panel c vs concentration of **5**.

Table 1. Enzyme Inhibition Efficacy of Compounds 1−6[a]

	IC_{50}			
	β-glucosidase		α-glucosidase	
compd	GBA1	GBA2	GAA	GANAB
1	165 ± 4 nM	139 ± 60 nM	>100 μM	>100 μM
2	304 ± 5 nM	14 ± 1 nM	>100 μM	>100 μM
3	>100 μM	>100 μM	15 ± 2 μM	>100 μM
4	21 ± 1 μM	>100 μM	38 ± 3 nM	1.4 ± 0.1 μM
5	>100 μM	>100 μM	82 ± 1 nM	29 ± 2 nM
6	119 ± 9.8 μM	58 ± 4.5 μM	>100 μM	>100 μM

[a]Apparent IC_{50} values for *in vitro* inhibition of GBA1, GBA2, GAA, and GANAB. Reported values are mean ± standard deviation from 3 technical replicates.

concentrations), limiting us to measuring a combined k_{inact}/K_I ratio for these molecules.

α-Cyclosulfate **5** displayed rapid pseudo first order inhibition kinetics against GAA (k_{inact}/K_I = 64 min^{-1} mM^{-1}), comparable to 1,6-*epi*-cyclophellitol aziridine **4** (Figure 3b,c, Table 2), illustrating the potency of α-configured cyclosulfates locked in a Michaelis complex conformation favoring nucleophilic interception. Conversely, irreversible inhibition of GBA1 by **6** was several orders of magnitude slower (K_I = 3.6 mM; k_{inact} = 0.015 min^{-1}; k_{inact}/K_I = 4.33 × 10^{-3} min^{-1} mM^{-1}), suggesting a limited ability of this molecule to adopt the $^1S_3$ conformation required for nucleophilic attack and β-glucosidase reactivity. Comparison of K_I values for **6** and **1** against GBA1 also showed initial binding of **6** to the enzyme to be substantially weaker compared to **1** (3.5 mM and 9 μM respectively). These values are consistent with the tighter binding affinities often displayed by TS shape analogues compared to molecules locked into other conformations.

Interestingly, while irreversible inhibition by aziridines **2** and **4** was largely specific toward α- or β-glucosidases respectively, these molecules were also observed to be less specific *reversible* inhibitors for glucosidases of the opposite anomeric specificity (competitive inhibition of GAA by **2**, K_I = 9.6 μM; competitive inhibition of GBA1 by **4**, K_I = 6.8 μM; Table 2). We reason that the common $^4H_3$ transition state utilized by both α- and β-glucosidases may allow these enzymes to bind aziridines of either "anomeric" configuration. Thus, the conformational preference of cyclophellitol cyclosulfates presents an advantage in specificity when compared to aziridine type inhibitors, by virtue of mimicking a reactive conformation receptive to nucleophilic attack, not shared between α- or β-glucosidases.

Structural Characterization of Enzyme−Cyclosulfate Interactions. Because of the key role of conformation in the contrasting inhibitory potency of cyclophellitol cyclosulfates

Table 2. Kinetic Parameters of Compounds 1−6[a]

	β-glucosidase GBA1			α-glucosidase GAA		
compd	k_{inact} (min^{-1})	K_I	k_{inact}/K_I (min^{-1} mM^{-1})	k_{inact} (min^{-1})	K_I	k_{inact}/K_I (min^{-1} mM^{-1})
1	0.72	9.2 μM	77.7		>500 μM	
2	nd	nd	19.0		9.6 μM*	
3		>500 μM		0.52	1.4 mM	0.37
4		6.8 μM*		nd	nd	58.0
5		>500 μM		nd	nd	64.3
6	0.015	3.6 mM	4.3 × 10^{-3}		>500 μM	

[a]Inactivation rates and inhibition constants (k_{inact} and K_I) for human recombinant β-glucosidase GBA1 and α-glucosidase GAA; nd, not determined due to fast inhibition; *, reversible inhibition observed.

DOI: 10.1021/acscentsci.7b00214
ACS Cent. Sci. 2017, 3, 784−793

against α- vs β-glucosidases, we set out to structurally characterize the conformational itinerary of **5** and **6** when reacted with representative bacterial glucosidases.

Crystal structures of **5** in complex with the GH31 α-glucosidase/tranglycosidase *Cj*Agd31B from *Cellvibrio japonicus*[10,31] were obtained by soaking crystals of wild type *Cj*Agd31B with **5**. We observed density for a covalent adduct bound to the enzyme nucleophile (Asp412) corresponding to ring opened cyclosulfate in a $^{1}S_{3}$ conformation (Figure 4a), matching the conformation previously observed for reacted aziridine **4**,[10] as well as a complex of *Cj*Agd31B reacted with 5-fluoro-α-glucosyl fluoride[31] (Figure 4b; PDB codes 5I24 and 4BA0 respectively). Structures of unreacted **5** were also obtained in complex with an inactive D412N nucleophile mutant of *Cj*Agd31B. Density for unreacted **5** in the *Cj*Agd31B active site matched a $^{4}C_{1}$ conformation as predicted by FEL calculations and NMR analysis (Figure 4a), demonstrating that **5** indeed binds to α-glucosidases as a conformational Michaelis complex analogue, allowing unimpeded access for in-line attack by the enzyme nucleophile. Difference density in the active site of *Cj*Agd31B D412N after soaking with **4** corresponded to an unreacted cyclophellitol aziridine in $^{4}H_{3}$ conformation (Figure 4b), consistent with this molecule acting as a TS shape mimic when unreacted.

We then utilized the β-glucosidase from *Thermoanaerobacterium xylanolyticum Tx*GH116 for structural studies with **6**. Due to its slow reactivity as an irreversible β-glucosidase inhibitor, we were able to capture an unreacted complex of **6** with crystals of wild type *Tx*GH116 by utilizing shorter ligand soaking times. After 10−20 min soaks, a single molecule of unreacted **6** was observed within the active site of *Tx*GH116, adopting a $^{4}C_{1}$ conformation in line with FEL calculations and NMR spectra. This $^{4}C_{1}$ conformation renders the equatorial C1−O bond of **6** poorly poised for in-line attack by the enzyme nucleophile Glu441, thus providing a structural rationale for the slow reactivity of this inhibitor against β-glucosidases. Extended ligand soaking times (~24 h) were required to produce a reacted covalent complex of **6** with *Tx*GH116. Reacted **6** was observed bound to the *Tx*GH116 catalytic nucleophile (Glu540) in a $^{4}C_{1}$ covalent intermediate conformation, consistent with the typical retaining β-glucosidase conformational itinerary utilized by this enzyme and matching the $^{4}C_{1}$ conformation previously observed for reacted 2-deoxy-2-fluoroglucoside (PDB code 5BX2).

We also investigated the structural basis for "off-target" inhibition by cyclophellitol aziridines, which we had observed to competitively inhibit glucosidases of "opposing" anomeric specificity. A crystal structure of **2** in complex with *Cj*Agd31B showed a single molecule of inhibitor occupying the enzyme active site, with the aziridine nitrogen H-bonding to the catalytic nucleophile carboxylate (~2.6 Å between aziridine N and Asp O Oδ; Figure S5). The presence of an unreacted aziridine between the nucleophile and the plane of the cyclitol ring induces an E_{3} conformation for the inhibitor, rather than the $^{4}H_{3}$ observed for an unreacted "correct" aziridine (Figure 4b). It is likely that the competitive inhibition of α-glucosidases by **4** is based around a similar interaction between the unreacted aziridine nitrogen and catalytic nucleophile.

Competitive ABPP of α-Glucosidases by Cyclosulfate 5. To assess the utility of cyclosulfates as enzyme inhibitors in complex biological samples, we examined the activity and selectivity of α-cyclosulfate **5** by competitive activity-based protein profiling (ABBP), against **13**[10] (Figure S1), a

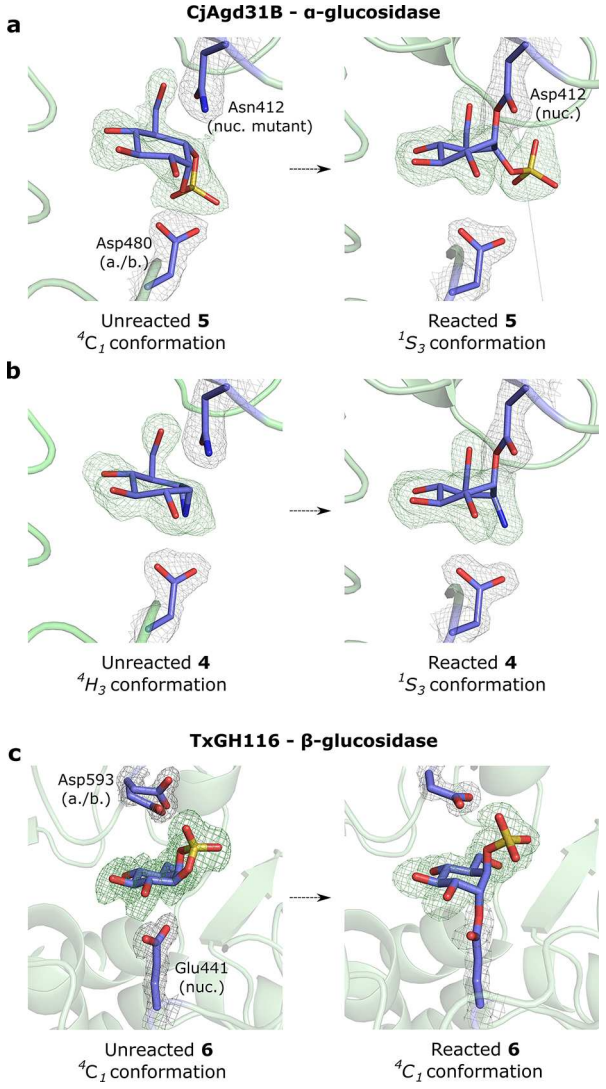

Figure 4. Structures of reacted **4** and **5** bound to wild type *Cj*Agd31B and reacted **6** bound to wild type *Tx*GH116. (a) Unreacted (left) and reacted (right) **5** in complex with *Cj*Agd31B D412N nucleophile mutant and wt *Cj*Agd31B respectively. Unreacted **5** adopts a $^{4}C_{1}$ ring conformation in the active site of *Cj*Agd31B, mimicking the Michaelis complex conformation of GH31 α-glucosidase substrates. Reacted **5** adopts a $^{1}S_{3}$ covalent intermediate conformation. (b) Unreacted (left) and reacted (right) **4** in complex with *Cj*Agd31B D412N nucleophile mutant and wt *Cj*Agd31B respectively. Unreacted **4** adopts a $^{4}H_{3}$ TS conformation. Reacted **4** adopts the same $^{1}S_{3}$ intermediate conformation as observed for **5**. (c) Unreacted (left) and reacted (right) β-cyclosulfate **6** with *Tx*GH116. Unreacted **6** in complex with GH116 β-glucosidase *Tx*GH116 adopts a $^{4}C_{1}$ conformation in the enzyme active site, which is poorly poised for attack by the enzyme nucleophile Glu441, and thus reacts extremely slowly. (Two conformations for the enzyme catalytic acid/base Asp593 can be seen in this complex.) Reacted **6** can be observed after extended soaking, and also adopts a $^{4}C_{1}$ conformation, covalently bound to the enzyme nucleophile. Electron density for protein side chains is *REFMAC* maximum-likelihood/σ_{A}-weighted $2F_{o} - F_{c}$ contoured to 0.44−0.51 and 0.40−0.42 electron/Å^{3} for *Cj*Agd31B and *Tx*GH116 complexes, respectively. Electron density for ligand is $F_{o} - F_{c}$ maps calculated just prior to building in ligand, contoured to 0.17−0.26 and 0.27−0.35 electron/Å^{3} for *Cj*Agd31B and *Tx*GH116 complexes, respectively. nuc. = nucleophile; a./b. = acid/base.

DOI: 10.1021/acscentsci.7b00214
ACS Cent. Sci. 2017, 3, 784−793

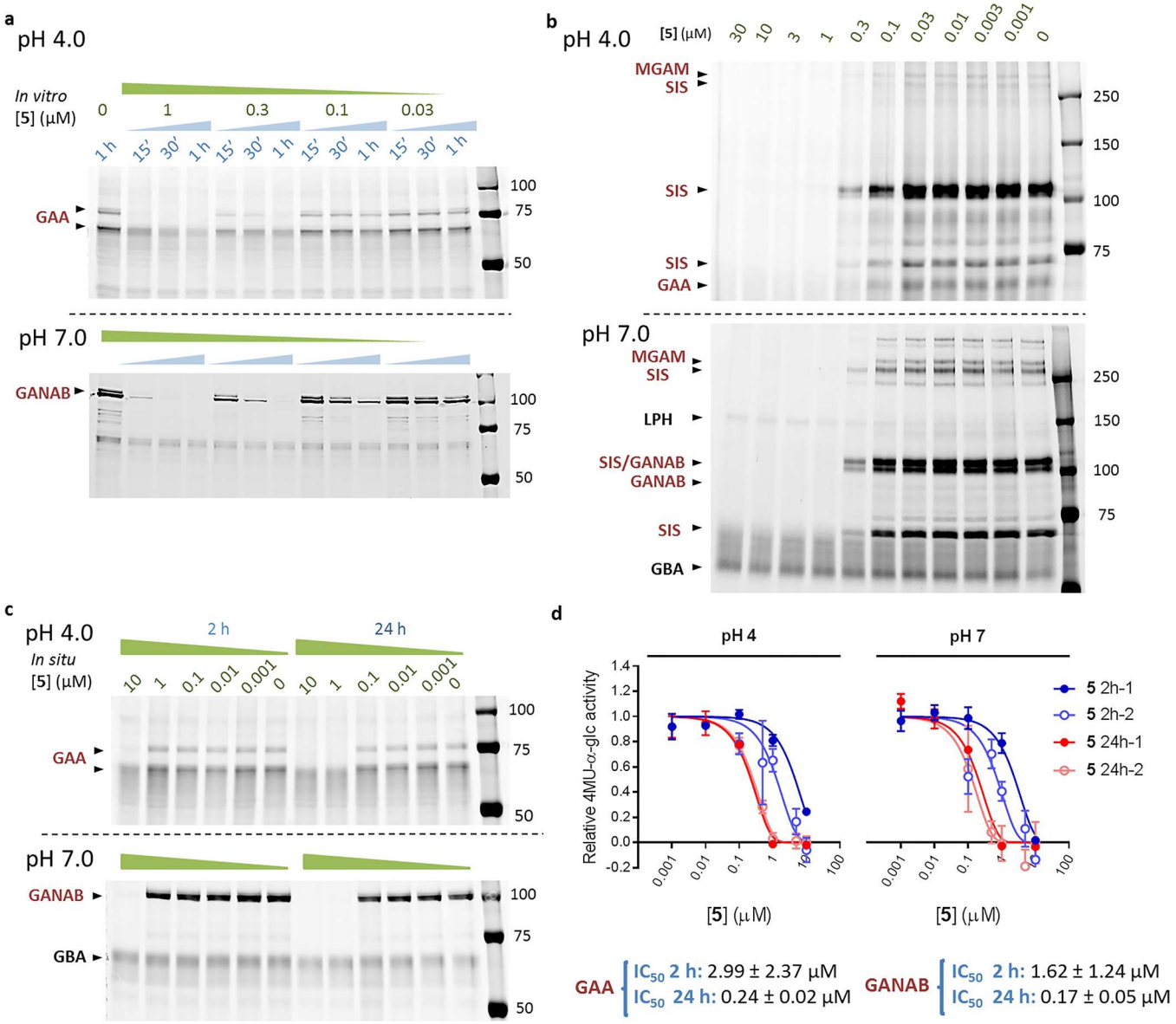

Figure 5. *In vitro* and *in situ* inhibition of GAA and GANAB. (a) **5** inhibits labeling of GAA and GANAB by fluorescent ABP **13** in fibroblast lysates in a concentration and time dependent manner. (b) **5** inhibits labeling of several α-glucosidases in mouse intestine lysate by **13**. Sucrase-isomaltase (Sis), maltase-glucoamylase (MGAM), GAA, and GANAB are labeled by **13**, as well as some off-target β-glucosidase labeling (LPH and GBA). α-Glucosidase labeling can be abrogated by preincubation with **5**, while β-glucosidase labeling persists, demonstrating the superior selectivity of **5** compared to **13**. (c) *In situ* inhibition of GAA and GANAB in fibroblasts at pH 4.0 and 7.0 respectively by **5** at incubation times of 2 and 24 h, followed by labeling of GAA and GANAB by cyclophellitol aziridine Cy5 probe **13**. (d) Apparent IC_{50}s for *in situ* inhibition of GAA and GANAB enzyme activity by **5**. Reported IC_{50}s are mean ± standard deviation from two biological replicates, each with three technical replicates.

fluorescent retaining α-glucosidase aziridine probe which labels GAA at pH 4 (isoforms at 70 and 76 kDa) and both isoforms of GANAB (~100 kDa) at pH 7.

We first preincubated fibroblast lysates with varying concentrations (1, 0.3, 0.1, and 0.03 μM) of **5** for 15, 30, or 60 min at pH 4 or pH 7, and subsequently labeled with **13** (1 μM) for 30 min. SDS−PAGE followed by fluorescence scanning showed time dependent inhibition of both GAA and GANAB by **5** at pH 4 and 7 respectively (Figure 5a). Competitive ABPP in GBA2 and GBA3 overexpressing HEK293T lysates (GBA2+ and GBA3+) against β-glucosidase probe **14** (Figure S1) showed no inhibition of retaining β-glucosidases by **5**, demonstrating the high selectivity of this inhibitor class (Figure S5).

Acarbose, miglitol, and voglibose are α-glucosidase inhibitors (AGIs) widely used in diabetes mellitus type II patients. These inhibitors delay the absorption of carbohydrates, decrease postprandial hyperglycemia and hyperinsulinemia, and thus improve insulin sensitivity and release stress on beta cells.[33−35] Prompted by the potential of AGIs as leads for diabetes mellitus type II drug development, we investigated the inhibition of a group of key metabolic α-glucosidases in murine gastrointestinal tract tissues using competitive ABPP. Our studies showed that, in addition to GAA and GANAB, **5** inhibited two α-glucosidases expressed specifically in intestinal tissue: sucrase-isomaltase (SIS) and maltase-glycoamylase (MGAM) (Figure 5b). Significantly, β-glucosidases lactase-phlorizin hydrolase (LPH) and GBA1, which are labeled in an off-target fashion by

DOI: 10.1021/acscentsci.7b00214
ACS Cent. Sci. 2017, 3, 784−793

13, are not outcompeted by preincubation with **5**, clearly demonstrating superior selectivity of cyclosulfate inhibitors compared to aziridines.

Lastly, we investigated whether α-cyclosulfate **5** is able to cross the cell membrane. Human fibroblasts were exposed to varying concentrations (10, 1, 0.1, 0.01, 0.001, and 0 μM) of **5** for 2 and 24 h, followed by extensive washing and lysate preparation. Lysates were incubated with **13** (0.5 μM) for 30 min and then separated by SDS−PAGE, followed by fluorescence scanning. Time dependent abrogation of ABP **13** fluorescence was observed, illustrating that **5** could cross the cell membrane to act *in situ* as α-glucosidase inhibitor (Figure 5c). Loss of ABP labeling was also accompanied by a corresponding loss of α-glucosidase enzymatic activity in harvested fibroblast lysates. Activity assays utilizing 4-methylumbelliferyl-α-glucose suggested robust *in situ* inhibition of both GAA and GANAB by **5**, with IC_{50}s of 3.0 and 1.6 μM respectively (Figure 5d).

CONCLUSION

In this study, we have presented a new class of irreversible glycosidase inhibitors: cyclophellitol cyclosulfates. We have shown that their irreversible action is specific for α- and β-glucosidases in a manner reflecting both the "anomeric" stereochemistry of the cyclophellitol cyclosulfates and the conformational itinerary of the target enzyme.

We have demonstrated, through *ab initio* metadynamics approaches and 3-D structures of enzyme ligand complexes, that unreacted α-cyclosulfate **5** favors a $^4C_1$ "Michaelis complex like" conformation which is perfectly poised for nucleophilic attack by α-glucosidases utilizing a $^4C_1 \rightarrow {}^4H_3 \rightarrow {}^1S_3$ glycosylation itinerary. Thus, **5** is a nanomolar mechanism-based retaining α-glucosidase inactivator, which follows pseudo first order kinetics, and displays superior selectivity compared to existing mechanism-based inhibitors due to its unique conformational behavior. We have also shown that **5** inhibits the intestinal retaining α-glucosidases SIS, MGAM, GAA, and GANAB, without affecting β-glucosidases intestinal LPH or GBA1. Thus, **5**, which is also able to cross the cell membrane, may be a good starting point for the development of agents for the treatment of type II diabetes.

β-Cyclosulfate **6** also adopts a $^4C_1$ conformation in its unreacted state, which does not match the $^1S_3$ conformation of typical β-glucosidase Michaelis complexes. When applied to retaining β-glucosidases following a $^1S_3 \rightarrow {}^4H_3 \rightarrow {}^4C_1$ conformational itinerary, **6** reacts extremely slowly compared to its congener **5**.

FEL calculations show that the ground state conformation of **6** is centered around $^4C_1$, a conformation with an equatorial C1−O bond that precludes in-line attack from the nucleophile. Crystal structures of unreacted **6** in complex with β-glucosidase *Tx*GH116 show that the β-cyclosulfate continues to adopt this $^4C_1$ conformation even within the enzyme active site. However, FEL calculations also suggest that it is energetically possible for **6** to access a TS-like $^4H_3$ conformation. Transient sampling of this TS conformation may allow for occasional reaction of **6** with β-glucosidases, as the cyclosulfate adopts a conformation better suited to nucleophilic attack by the enzyme. However, the slow rate of irreversible inhibition observed for **6** suggests that its predominant conformation within the enzyme active site is one where nucleophilic attack from the enzyme is disfavored.

The last 10−20 years have provided us a deep appreciation of reaction coordinates of diverse glycosidases.[6,7,10,36] This conformational canvas inspires the design and application of chemical species to mimic specific species along the reaction coordinate. Much existing work has focused on the design of noncovalent transition state mimics, or conformationally restricted species that mimic a species along only certain reaction trajectories, such as the specific inhibition of GH47 α-mannosidases by kifunensine.[37,38] Recent years have, however, seen a resurgence in the development of irreversible enzyme inhibitors as clinical probes and diagnostics.[10,11,16,39] With such applications in mind, the development of conformationally restrained irreversible inhibitors primed for nucleophilic attack through mimicry of the Michaelis complex, coupled to more electrophilic reaction centers, inspires creation of conceptually new, potent and selective glycosidase inhibitors. We envision that our design strategy will also be applied for other glycosidases, both those following a similar $^4C_1 \rightarrow {}^4H_3 \rightarrow {}^1S_3$ conformational itinerary and those following other conformational trajectories, guided by the conformational preference of the reaction pathway.

MATERIALS AND METHODS

All chemicals were obtained from Sigma-Aldrich, unless otherwise stated. Pompe disease fibroblasts, HEK293T cells (ATCC-CRL-3216), and normal fibroblast cell lines were obtained from the American Type Culture Collection (ATCC) and transfected for GBA2 and GBA3 overexpression (Supporting Information). Cell lines were cultured in DMEM/F-12 (Ham) medium (Invitrogen) supplemented with 10% (v/v) fetal calf serum (FCS; Sigma) and 1% penicillin/streptomycin (Sigma). Mouse tissues were isolated according to guidelines approved by the ethical committee of Leiden University (DEC#13191). Human recombinant enzymes rGBA1 (Cerezyme) and rGAA (Myozyme) were donated by Genzyme, GBA2 was overexpressed in HEK293T lysates, and GANAB was obtained from fibroblasts of Pompe patients diagnosed on the basis of absence of GAA (Supporting Information). Bacterial enzymes *Tm*GH1,[29] *Tx*GH116,[30] and *Cj*Agd31B[31] were expressed as previously described. All cell or tissue lysates were prepared in KPI buffer (25 mM potassium phosphate pH 6.5, supplemented with protease inhibitor 1× cocktail (Roche)) via homogenization on ice with SilentCrusher S equipped with Typ 7 F/S head (30 × 1000 rpm, 3 × 7 s). Lysate protein concentrations were determined with BCA Protein Assay Kit (Pierce). Lysates and proteins were stored in small aliquots at −80 °C until use.

IC_{50} and Inhibition Kinetics Determination. Detailed protocols for IC_{50} and inhibition kinetics measurements can be found in the Supporting Information.

In brief, apparent IC_{50} values were determined by preincubating enzymes with a range of inhibitor concentrations in a 25 μL volume for 30 min at 37 °C (for human enzymes) or 25 °C (for bacterial enzymes). Following preincubation, 25 μL of the enzyme−inhibitor mixture was transferred into 100 μL of the appropriate 4-MU−Glc substrate mixture to determine residual activity. Reactions were quenched with 1 M NaOH−glycine (pH 10.3) upon completion, and 4-MU fluorescence was measured with a LS55 fluorescence spectrophotometer (PerkinElmer) (λ_{EX} 366 nm; λ_{EM} 445 nm). IC_{50} values reported are the mean values from three technical replicates.

In situ IC_{50} values were determined by incubating normal human dermal fibroblasts (grown to confluency) with **5** for 2

DOI: 10.1021/acscentsci.7b00214
ACS Cent. Sci. 2017, 3, 784−793

and 24 h. Cells were washed three times with PBS and harvested by scraping into KPI buffer supplemented with 0.1% (v/v) Triton X-100 and 1× cOmplete protease inhibitor cocktail (Roche). Residual GAA and GANAB activity was measured on the basis of hydrolysis of 4-MU−α-Glc at pH 4 or 7. *In situ* IC_{50} values are mean values from two biological replicates, each with 3 technical repeats (Figure 5d).

For kinetics, enzyme and relevant concentrations of inhibitor were preincubated for 0.5, 2, 3.5, 5, and 8 min for fast inhibitors and 0.5, 20, 60, 120, 180, 240, and 360 min for slow inhibitors. At relevant time points, 5 μL of this enzyme−inhibitor mixture was added to 2,4-DNP−Glc substrate, and release of 2,4-dinitrophenolate was monitored via absorbance at 400 nm to determine the rate of hydrolysis after inhibition (V) compared to a no inhibitor control (V_0).

Pseudo first order rate constants (k_{obs}) were obtained from a linear fit of $-\ln V/V_0$ against time for each value of [I]. A plot of k_{obs} against [I] fitted to the hyperbolic equation $k_{obs} = (k_{inact}[I]/K_I + [I])$ was used to determine k_{inact} and K_I. Where fast inhibition was observed (>50% after 30 s), the k_{inact}/K_I ratio was determined at low values of [I] ($\ll K_I$), using the approximation $k_{obs} \approx k_{inact}[I]/K_I$, where k_{inact}/K_I is the slope of a linear fit of k_{obs} vs [I]. Where reversible inhibition was observed (no variation of $-\ln V/V_0$ with time), K_I was determined by use of Lineweaver−Burk plots at different values of [I].

Time and Concentration Dependent *in Vitro* Inhibition of GAA and GANAB. Homogenates of human normal dermal fibroblast (17.6 μg total protein) were preincubated on ice for 5 min in 150 mM McIlvaine buffer pH 4 or 7 in a total volume of 10 μL. Samples were then incubated for 15, 30, and 60 min at 37 °C with 2.5 μL inhibitor dilutions in McIlvaine buffer pH 4 or 7 to obtain a final concentration of 5, 1.5, 0.5, 0.15, and 0 μM. Afterward, the samples were further incubated with 2.5 μL of ABP **13** (1 μM), diluted in McIlvaine buffer pH 4 or 7 for 30 min at 37 °C. Finally, samples were denatured with 5 μL of 4× Laemmli sample buffer for 5 min at 98 °C, and resolved by 10% (w/v) SDS−PAGE. Wet slab gels were subjected to Cy5 fluorescence scaning (Typhoon FLA9500, GE, $\lambda_{EX} \geq 635$ nm, $\lambda_{EM} \geq 665$ nm).

***In Vitro* Inhibition of α-Glucosidases in Mouse Gastrointestinal Lysate.** Mixtures of mouse duodenum, jejunum, and ileum homogenates containing 40 μg total protein were incubated on ice for 5 min with McIlvaine buffer at pH 4 or 7, in a total volume of 10 μL. Samples were subsequently incubated with 2.5 μL of **5** for 1 h at 37 °C at various inhibitor dilutions in McIlvaine buffer at pH 4.0 or 7.0 to obtain a final concentration of 150, 50, 15, 5, 1.5, 0.5, 0.15, 0.05, 0.015, 0.005, and 0 μM. Then, the samples were further incubated with 2.5 μL of **13** (6 μM, diluted in McIlvaine buffer at pH 4.0 or 7.0) for 30 min at 37 °C. Samples were denatured by boiling with 3.75 μL of 4× Laemmli sample buffer for 5 min, and resolved by 10% (w/v) SDS−PAGE. Wet slab gels were subjected to Cy5 fluorescence scanning (Typhoon FLA9500, GE, $\lambda_{EX} \geq 635$ nm, $\lambda_{EM} \geq 665$ nm).

***In Situ* inhibition of GAA and GANAB.** Human normal dermal fibroblasts were grown to confluence and *in situ* treated with inhibitor **5** at various concentrations (10, 1, 0.1, 0.01, 0.001, and 0 μM) in duplicates for 2 or 24 h. Cells were harvested by first washing three times with PBS and subsequently lysed with KPI buffer (25 mM K_2HPO_4/KH_2PO_4, pH 6.5, 0.1% (v/v) Triton X-100, protease inhibitor cocktail (Roche)) on ice for 30 min. Homogenates were collected by scraping, vortexed, and stored at −80 °C. Lysates containing 4 μg total protein were equilibrated to pH 4 or 7 in 150 mM McIlvaine buffer for 5 min on ice, and incubated with probe **13** (0.5 μM) for 30 min at 37 °C at either pH 4 or 7 in a total volume of 15 μL. Samples were denatured, resolved by SDS−PAGE, and subjected to fluorescent scan (Typhoon FLA9500, GE, $\lambda_{EX} \geq 635$ nm, $\lambda_{EM} \geq 665$ nm)

■ ASSOCIATED CONTENT

Supporting Information

The Supporting Information is available free of charge on the ACS Publications website at DOI: 10.1021/acscentsci.7b00214.

Synthesis and characterization of **5** and **6**, synthesis of all intermediates, molecular modeling, labeling of glucosidases, SDS−PAGE analysis and fluorescence scanning, and crystallographic data collection and refinement statistics (PDF)

■ AUTHOR INFORMATION

Corresponding Authors

*E-mail: gideon.davies@york.ac.uk.
*E-mail: h.s.overkleeft@chem.leidenuniv.nl.

ORCID

Marta Artola: 0000-0002-3051-3902
Jeroen D. C. Codée: 0000-0003-3531-2138
Carme Rovira: 0000-0003-1477-5010
Gideon J. Davies: 0000-0002-7343-776X
Herman S. Overkleeft: 0000-0001-6976-7005

Author Contributions

M.A. synthesized the inhibitors under the guidance of J.D.C.C. and G.A.v.d.M. M.A., M.J.F., and C.-L.K. conducted the enzyme inhibition and biochemistry assays under the guidance of J.M.F.G.A.. L.W., W.A.O., I.Z.B., and G.J.D. designed and performed the X-ray diffraction experiments. L.R. performed metadynamics simulations under guidance of C.R. H.S.O. and G.J.D. conceived the idea, supervised the project, and with M.A. and L.W. wrote the manuscript.

Notes

The authors declare no competing financial interest.

■ ACKNOWLEDGMENTS

We thank The Netherlands Organization for Scientific Research (NWO-CW, ChemThem grant to J.M.F.G.A. and H.S.O.), the European Research Council (ERC-2011-AdG-290836 "Chembiosphing", to H.S.O., and ERC-2012-AdG-322942 "Glycopoise", to G.J.D.), Sanofi Genzyme (research grant to J.M.F.G.A. and H.S.O. and postdoctoral contract to M.A.), the Spanish Ministry of Economy and Competitiveness (CTQ2014-55174-P), and the Generalitat de Catalunya (2014SGR-987) for financial support. We thank the Diamond Light Source for access to beamline i02 and i04 (proposal number mx-13587) and the Barcelona Supercomputing Center (BSC-CNS, RES-QCM-2017-1-00014) for technical support and computational resources provided, which contributed to the results presented here. L.R. acknowledges a Ph.D. fellowship from the University of Barcelona (APIF-UB). G.J.D. is supported by the Royal Society though the Ken Murray Research Professorship.

DOI: 10.1021/acscentsci.7b00214
ACS Cent. Sci. 2017, 3, 784−793

REFERENCES

(1) Lombard, V.; Ramulu, H. G.; Drula, E.; Coutinho, P. M.; Henrissat, B. The carbohydrate-active enzymes database (CAZy) in 2013. *Nucleic Acids Res.* **2014**, *42*, D490−D495.

(2) Jongkees, S. A. K.; Withers, S. G. Unusual Enzymatic Glycoside Cleavage Mechanisms. *Acc. Chem. Res.* **2014**, *47*, 226−235.

(3) Gloster, T. M.; Davies, G. J. Glycosidase inhibition: assessing mimicry of the transition state. *Org. Biomol. Chem.* **2010**, *8*, 305−20.

(4) Vasella, A.; Davies, G. J.; Bohm, M. Glycosidase mechanisms. *Curr. Opin. Chem. Biol.* **2002**, *6*, 619−629.

(5) Vocadlo, D. J.; Davies, G. J. Mechanistic insights into glycosidase chemistry. *Curr. Opin. Chem. Biol.* **2008**, *12*, 539−555.

(6) Ardevol, A.; Rovira, C. Reaction Mechanisms in Carbohydrate-Active Enzymes: Glycoside Hydrolases and Glycosyltransferases. Insights from ab Initio Quantum Mechanics/Molecular Mechanics Dynamic Simulations. *J. Am. Chem. Soc.* **2015**, *137*, 7528−7547.

(7) Davies, G. J.; Williams, S. J. Carbohydrate-active enzymes: sequences, shapes, contortions and cells. *Biochem. Soc. Trans.* **2016**, *44*, 79−87.

(8) Kallemeijn, W. W.; Witte, M. D.; Wennekes, T.; Aerts, J. M. Mechanism-based inhibitors of glycosidases: design and applications. *Adv. Carbohydr. Chem. Biochem.* **2014**, *71*, 297−338.

(9) Beenakker, T. J. M.; Wander, D. P. A.; Offen, W. A.; Artola, M.; Raich, L.; Ferraz, M. J.; Li, K. Y.; Houben, J.; van Rijssel, E. R.; Hansen, T.; van der Marel, G. A.; Codee, J. D. C.; Aerts, J.; Rovira, C.; Davies, G. J.; Overkleeft, H. S. Carba-cyclophellitols Are Neutral Retaining-Glucosidase Inhibitors. *J. Am. Chem. Soc.* **2017**, *139*, 6534−6537.

(10) Speciale, G.; Thompson, A. J.; Davies, G. J.; Williams, S. J. Dissecting conformational contributions to glycosidase catalysis and inhibition. *Curr. Opin. Struct. Biol.* **2014**, *28*, 1−13.

(11) Witte, M. D.; Kallemeijn, W. W.; Aten, J.; Li, K. Y.; Strijland, A.; Donker-Koopman, W. E.; van den Nieuwendijk, A. M.; Bleijlevens, B.; Kramer, G.; Florea, B. I.; Hooibrink, B.; Hollak, C. E.; Ottenhoff, R.; Boot, R. G.; van der Marel, G. A.; Overkleeft, H. S.; Aerts, J. M. Ultrasensitive in situ visualization of active glucocerebrosidase molecules. *Nat. Chem. Biol.* **2010**, *6*, 907−913.

(12) Jiang, J.; Beenakker, T. J.; Kallemeijn, W. W.; van der Marel, G. A.; van den Elst, H.; Codee, J. D.; Aerts, J. M.; Overkleeft, H. S. Comparing Cyclophellitol *N*-Alkyl and *N*-Acyl Cyclophellitol Aziridines as Activity-Based Glycosidase Probes. *Chem. - Eur. J.* **2015**, *21*, 10861−10869.

(13) Withers, S. G.; Umezawa, K. Cyclophellitol: a naturally occurring mechanism-based inactivator of beta-glucosidases. *Biochem. Biophys. Res. Commun.* **1991**, *177*, 532−537.

(14) Gloster, T. M.; Madsen, R.; Davies, G. J. Structural basis for cyclophellitol inhibition of a beta-glucosidase. *Org. Biomol. Chem.* **2007**, *5*, 444−446.

(15) Willems, L. I.; Beenakker, T. J.; Murray, B.; Scheij, S.; Kallemeijn, W. W.; Boot, R. G.; Verhoek, M.; Donker-Koopman, W. E.; Ferraz, M. J.; van Rijssel, E. R.; Florea, B. I.; Codee, J. D.; van der Marel, G. A.; Aerts, J. M.; Overkleeft, H. S. Potent and selective activity-based probes for GH27 human retaining alpha-galactosidases. *J. Am. Chem. Soc.* **2014**, *136*, 11622−11625.

(16) Jiang, J. B.; Kallemeijn, W. W.; Wright, D. W.; van den Nieuwendijk, A. M. C. H.; Rohde, V. C.; Folch, E. C.; van den Elst, H.; Florea, B. I.; Scheij, S.; Donker-Koopman, W. E.; Verhoek, M.; Li, N.; Schurmann, M.; Mink, D.; Boot, R. G.; Codee, J. D. C.; van der Marel, G. A.; Davies, G. J.; Aerts, J. M. F. G.; Overkleeft, H. S. In vitro and in vivo comparative and competitive activity-based protein profiling of GH29 alpha-L-fucosidases. *Chem. Sci.* **2015**, *6*, 2782−2789.

(17) Li, K. Y.; Jiang, J.; Witte, M. D.; Kallemeijn, W. W.; Donker-Koopman, W. E.; Boot, R. G.; Aerts, J. M.; Codee, J. D.; van der Marel, G. A.; Overkleeft, H. S. Exploring functional cyclophellitol analogues as human retaining beta-glucosidase inhibitors. *Org. Biomol. Chem.* **2014**, *12*, 7786−7791.

(18) Gao, Y.; Sharpless, K. B. Vicinal Diol Cyclic Sulfates - Like Epoxides Only More Reactive. *J. Am. Chem. Soc.* **1988**, *110*, 7538−7539.

(19) Ernst, B.; Magnani, J. L. From carbohydrate leads to glycomimetic drugs. *Nat. Rev. Drug Discovery* **2009**, *8*, 661−677.

(20) Atsumi, S.; Umezawa, K.; Iinuma, H.; Naganawa, H.; Nakamura, H.; Iitaka, Y.; Takeuchi, T. Production, isolation and structure determination of a novel beta-glucosidase inhibitor, cyclophellitol, from Phellinus sp. *J. Antibiot.* **1990**, *43*, 49−53.

(21) Tatsuta, K.; Niwata, Y.; Umezawa, K.; Toshima, K.; Nakata, M. Syntheses and enzyme inhibiting activities of cyclophellitol analogs. *J. Antibiot.* **1991**, *44*, 912−914.

(22) McCarter, J. D.; Withers, S. G. 5-fluoro glycosides: A new class of mechanism-based inhibitors of both alpha- and beta-glucosidases. *J. Am. Chem. Soc.* **1996**, *118*, 241−242.

(23) Withers, S. G.; Street, I. P.; Bird, P.; Dolphin, D. H. 2-Deoxy-2-Fluoroglucosides - a Novel Class of Mechanism-Based Glucosidase Inhibitors. *J. Am. Chem. Soc.* **1987**, *109*, 7530−7531.

(24) Rempel, B. P.; Withers, S. G. Covalent inhibitors of glycosidases and their applications in biochemistry and biology. *Glycobiology* **2008**, *18*, 570−586.

(25) Laio, A.; Parrinello, M. Escaping free-energy minima. *Proc. Natl. Acad. Sci. U. S. A.* **2002**, *99*, 12562−12566.

(26) Hansen, F. G.; Bundgaard, E.; Madsen, R. A short synthesis of (+)-cyclophellitol. *J. Org. Chem.* **2005**, *70*, 10139−10142.

(27) Li, K.-Y.; Jiang, J.; Witte, M. D.; Kallemeijn, W. W.; van den Elst, H.; Wong, C.-S.; Chander, S. D.; Hoogendoorn, S.; Beenakker, T. J. M.; Codée, J. D. C.; Aerts, J. M. F. G.; van der Marel, G. A.; Overkleeft, H. S. Synthesis of Cyclophellitol, Cyclophellitol Aziridine, and Their Tagged Derivatives. *Eur. J. Org. Chem.* **2014**, *2014*, 6030−6043.

(28) Jiang, J.; Kuo, C. L.; Wu, L.; Franke, C.; Kallemeijn, W. W.; Florea, B. I.; van Meel, E.; van der Marel, G. A.; Codee, J. D.; Boot, R. G.; Davies, G. J.; Overkleeft, H. S.; Aerts, J. M. Correction to "Detection of Active Mammalian GH31 alpha-Glucosidases in Health and Disease Using In-Class, Broad-Spectrum Activity-Based Probes". *ACS Cent. Sci.* **2016**, *2*, 351−358.

(29) Gloster, T. M.; Meloncelli, P.; Stick, R. V.; Zechel, D.; Vasella, A.; Davies, G. J. Glycosidase inhibition: An assessment of the binding of 18 putative transition-state mimics. *J. Am. Chem. Soc.* **2007**, *129*, 2345−2354.

(30) Charoenwattanasatien, R.; Pengthaisong, S.; Breen, I.; Mutoh, R.; Sansenya, S.; Hua, Y.; Tankrathok, A.; Wu, L.; Songsiriritthigul, C.; Tanaka, H.; Williams, S. J.; Davies, G. J.; Kurisu, G.; Cairns, J. R. Bacterial Beta-Glucosidase Reveals the Structural and Functional Basis of Genetic Defects in Human Glucocerebrosidase 2 (GBA2). *ACS Chem. Biol.* **2016**, *11*, 1891−1900.

(31) Larsbrink, J.; Izumi, A.; Hemsworth, G. R.; Davies, G. J.; Brumer, H. Structural Enzymology of Cellvibrio japonicus Agd31B Protein Reveals alpha-Transglucosylase Activity in Glycoside Hydrolase Family 31. *J. Biol. Chem.* **2012**, *287*, 43288−43299.

(32) Islam, M. R.; Grubb, J. H.; Sly, W. S. C-terminal processing of human beta-glucuronidase. The propeptide is required for full expression of catalytic activity, intracellular retention, and proper phosphorylation. *J. Biol. Chem.* **1993**, *268*, 22627−22633.

(33) Scheen, A. J. Is there a role for alpha-glucosidase inhibitors in the prevention of type 2 diabetes mellitus? *Drugs* **2003**, *63*, 933−951.

(34) van de Laar, F. A.; Lucassen, P. L.; Akkermans, R. P.; van de Lisdonk, E. H.; Rutten, G. E.; van Weel, C. Alpha-glucosidase inhibitors for patients with type 2 diabetes: results from a Cochrane systematic review and meta-analysis. *Diabetes Care* **2005**, *28*, 154−163.

(35) Wardrop, D. J.; Waidyarachchi, S. L. Synthesis and biological activity of naturally occurring alpha-glucosidase inhibitors. *Nat. Prod. Rep.* **2010**, *27*, 1431−1468.

(36) Davies, G. J.; Planas, A.; Rovira, C. Conformational analyses of the reaction coordinate of glycosidases. *Acc. Chem. Res.* **2012**, *45*, 308−316.

(37) Vallee, F.; Karaveg, K.; Herscovics, A.; Moremen, K. W.; Howell, P. L. Structural basis for catalysis and inhibition of *N*-glycan processing class I alpha 1,2-mannosidases. *J. Biol. Chem.* **2000**, *275*, 41287−41298.

DOI: 10.1021/acscentsci.7b00214
ACS Cent. Sci. 2017, 3, 784−793

(38) Thompson, A. J.; Dabin, J.; Iglesias-Fernandez, J.; Ardevol, A.; Dinev, Z.; Williams, S. J.; Bande, O.; Siriwardena, A.; Moreland, C.; Hu, T. C.; Smith, D. K.; Gilbert, H. J.; Rovira, C.; Davies, G. J. The reaction coordinate of a bacterial GH47 alpha-mannosidase: a combined quantum mechanical and structural approach. *Angew. Chem., Int. Ed.* **2012**, *51*, 10997−11001.
(39) Schultheis, P. J.; Fleming, S. M.; Clippinger, A. K.; Lewis, J.; Tsunemi, T.; Giasson, B.; Dickson, D. W.; Mazzulli, J. R.; Bardgett, M. E.; Haik, K. L.; Ekhator, O.; Chava, A. K.; Howard, J.; Gannon, M.; Hoffman, E.; Chen, Y.; Prasad, V.; Linn, S. C.; Tamargo, R. J.; Westbroek, W.; Sidransky, E.; Krainc, D.; Shull, G. E. Atp13a2-deficient mice exhibit neuronal ceroid lipofuscinosis, limited alpha-synuclein accumulation and age-dependent sensorimotor deficits. *Hum. Mol. Genet.* **2013**, *22*, 2067−2082.

DOI: 10.1021/acscentsci.7b00214
ACS Cent. Sci. 2017, 3, 784−793